

Available online at www.sciencedirect.com ScienceDirect

Procedia Engineering 2 (2010) 2381–2386

**Procedia
Engineering**

www.elsevier.com/locate/procedia8th Conference of the International Sports Engineering Association (ISEA)

Ski jumping flight skill analysis based on high-speed video image

Masahide Murakami^{a, *}, Masato Iwase^a, Kazuya Seo^b, Yuji Ohgi^c and Reno Koyanagi^c^aGraduate School of Systems and Information Engineering, University of Tsukuba, Tsukuba-city 305-8573 Japan^bFaculty of Education, Art and Science, Yamagata University, Yamagata 990-8560 Japan^cGraduate School of Media and Governance, Keio University, Fujisawa 252-8520 Japan*

Received 31 January 2010; revised 7 March 2010; accepted 21 March 2010

Abstract

Images of the initial 40 m part of a flight of 120-m ski jumping were recorded by a fixed high-speed video camera in Hakuba Ski Jumping Stadium. The time variations of the forward leaning angle and the ski angle of attack were measured from the video image and the aerodynamic forces were calculated from kinematic data. Some correlations were investigated between the reduced jumping distance D_r , which is an initial speed corrected flight distance, and some key angles and the initial transition time, as well as those between D_r and the aerodynamic force coefficients. Jumping performance is compared between advanced jumpers and beginner jumpers.

© 2010 Published by Elsevier Ltd. Open access under [CC BY-NC-ND license](http://creativecommons.org/licenses/by-nc-nd/3.0/).*Keywords:* Ski jumping, image analysis, flight distance, jumper posture, aerodynamic force coefficients

1. Introduction

Ski jumping, in particular the flight phase, can be quantitatively treated from the aerodynamics point of view. Some wind tunnel experiments [1,2] and field experiments based on video image analysis have been conducted for maximum flight distance and safety. The wind tunnel test for a V-style flight was conducted, and a database for the aerodynamic force coefficients was constructed by Seo et al. [3]. It was further used in the jumping flight optimization study [4]. The attempt to derive the aerodynamic forces was also performed on the basis of the image analysis of high-speed video image of real jumping flight [5,6]. It seems the method of image analysis for video images of real jumping flights was basically established [6]. In this study the image analysis method was further improved for higher accuracy by executing detailed on-site survey of the jumping field, Hakuba Jumping Stadium, and by applying a highly accurate image correction method based on the survey data. As a result, the accuracy was considerably improved, and, furthermore, large amount of data have been accumulated for statistical data treatment. We calculated some correlations between the flight distance and some angles of jumper posture, and between flight

* Corresponding author. Tel.: +81-29-836-7168; fax: +81-29-836-7168.
E-mail address: aml05216@mail1.accsnet.ne.jp

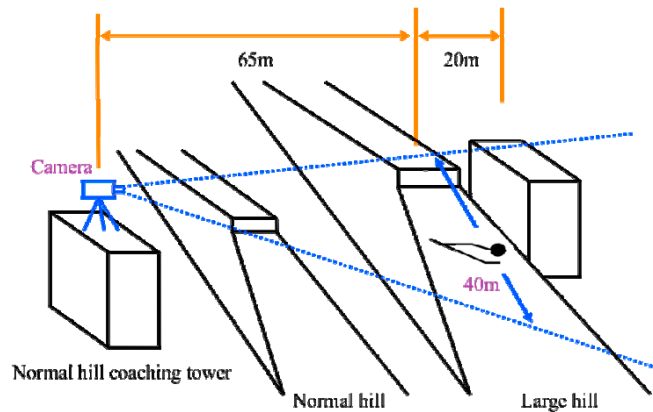


Fig. 1. Sketch of the video camera installation place

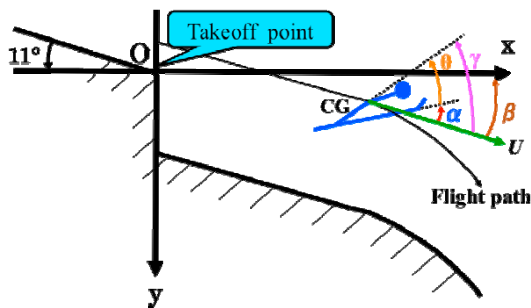


Fig. 2. Coordinate system and the definition of angles

distance and the aerodynamic force coefficients based on the large amount of data. The primary factors that strongly influence the jumping flight are determined from the examination of these correlation data.

2. Acquisition of High-Speed Video Image and Image Analysis

The flights of large-hill class jumping were recorded with a high-speed video set on the top of the coaching tower of the normal-hill jumping as shown in Fig. 1. The location of the camera is about 15 m downward along the large-hill landing slope from the take-off point and 65 m away from the large-hill landing slope. The detail was described in our previous report [6]. The field of view of the camera with a wide-angle lens with a focal length of 28 mm covers upper 40 m range of the landing slope. This roughly corresponds to a flight for initial 2 s. The video camera was operated at 250 frames/s. The subjects in these tests included Japanese Olympic team jumpers, university and high school jumpers and a number of World Cup high-ranking jumpers. As no wind data were available, the effect of wind was ignored. As a matter of fact, wind was weak to moderate during the tests. The coordinate system, and the centre of gravity (CG) and the angles characterizing the posture of a jumper are shown in Fig. 2. The coordinate origin is the take-off point, and the y-axis is taken vertically downward.

The center of gravity of a flying jumper is pursued in the images to derive the velocity and acceleration. In this study, the CG value was calculated as a weighted average of the positions of the waist, head and toe. The specific weights of body segments of a jumper were calculated by referring to the paper [7]. The mass of a jumper was assumed to be 70 kg including ski. The image tracking for these selected positions was mostly accomplished automatically with the aid of image analysis software, but partly with some manual assist for cases where the positions were hard to be distinguished because they seemed as if they were blended into the background.

A single fixed video camera with a wide-angle lens was used instead of adopting a three-dimensional camera system. Some image distortion that is unavoidable in our camera system must be corrected before the image analysis. For this purpose, site survey had been executed in advance.

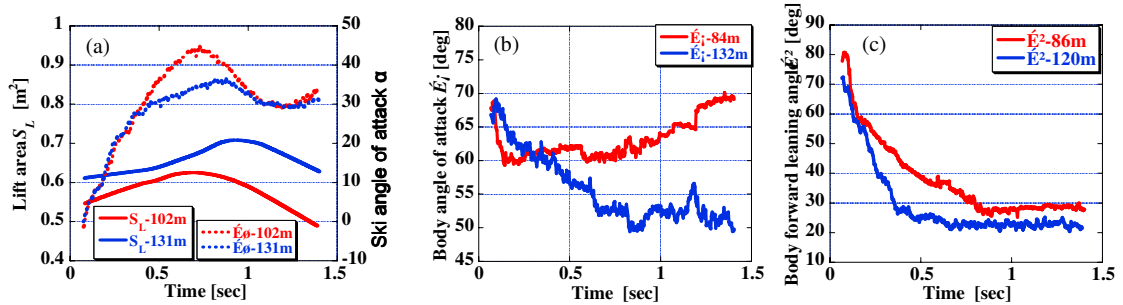


Fig. 3. Time variations of the lift area S_L and some angles of a jumper posture for two typical cases (an advanced jumper and a beginner). (a) for lift area S_L and the ski angle of attack α , (b) for the body angle of attack γ , and (c) for the body forward leaning angle θ .

Then, we took the images of staffs with four markers with an interval of 1 m put up exactly on the survey points on the landing slope by the video camera under the same condition as the jump image recording. Thus, total 96 points were used for the image correction. Based on these points in the images, of which coordinate values are known, we constructed a conversion formula from the pixel coordinate to the physical coordinate. They are polynomials of degree 2 of x and y for the x-direction correction, and of degree 4 for the y-direction correction. For the data analysis, the first and the second order time derivatives of CG data should be computed for the velocity and acceleration, from which the aerodynamic forces are derived. High-accuracy numerical differentiation scheme is adopted for the velocity and acceleration calculations.

$$\frac{df}{dt} = \frac{-f_{+2} + 8f_{+1} - 8f_{-1} + f_{-2}}{12\Delta t} \tag{1}$$

It is, however, seen that some data smoothing procedures are further required for the significant derivation of the velocity and acceleration. The low pass filtering with a cut-off frequency of 3 Hz and the weighted least square regression with a higher order polynomial are introduced for this purpose.

3. Results and Discussion

3.1. Derivation of aerodynamic force coefficients and angles characterizing a jumper posture

The aerodynamic forces, the lift L and the drag D , are computed in terms of the accelerations, a_x and a_y , and the flight angle β after the effect of gravity g is subtracted.

$$L = m \left[a_x \sin \beta - (a_y - g) \cos \beta \right] \tag{2}$$

$$D = -m \left[a_x \cos \beta + (a_y - g) \sin \beta \right] \tag{3}$$

where m is the jumper mass. The lift area S_L and the drag area S_D are conventionally used instead of the lift coefficient and the drag coefficient because the projected area of a jumper largely changes during a flight [1-3].

$$S_L = 2L / \rho U^2 \tag{4}$$

$$S_D = 2D / \rho U^2 \tag{5}$$

where ρ is the air density.

The time variations of S_L and the ski angle of attack α are shown in Fig. 3 (a) for two ski jumpers, a Japanese A-class jumper (flight distance of 131 m) and a high school jumper (102 m). The take-off speed was almost equal for the two cases. It is seen that S_L is larger for the A-class jumper than that of high school jumper throughout the

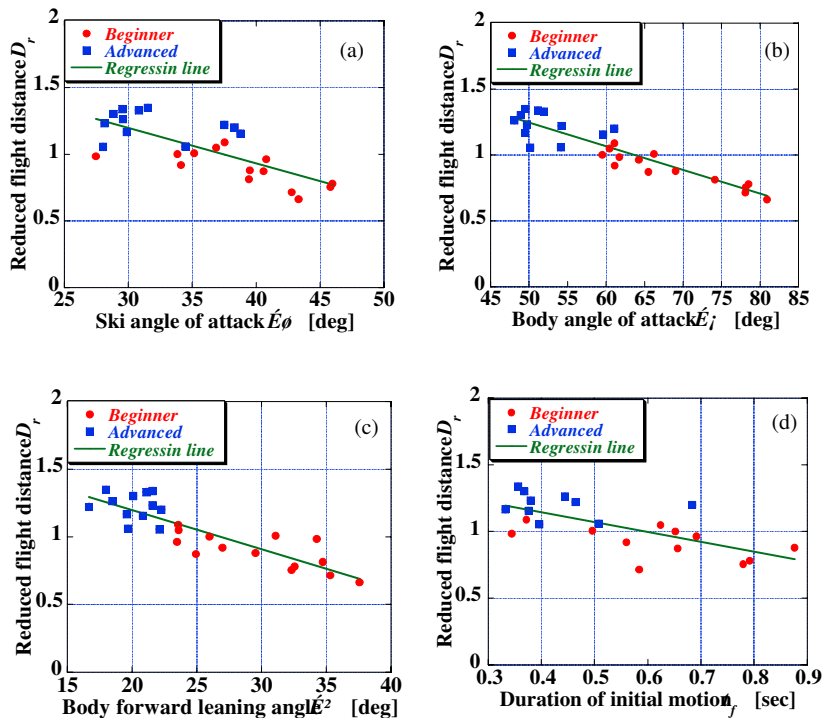


Fig. 4 Correlation results, (a) for α - D_r correlation, (b) for γ - D_r correlation, (c) for θ - D_r correlation and (d) for t_f - D_r correlation. Closed blue squares are the data for advanced jumpers (World Cup ranking jumpers and Japanese A-class jumpers) and red circles for beginner (high school and university students) jumpers. The green solid line is a linear least square regression line for all the data.

record. It is interesting to note that S_L begins to decrease a little before 1 s for the A-class jumper and 0.7 s for the high school jumper. This must be a symptom of aerodynamic stall. The stall started earlier for the high school jumper because of larger α caused by pitching of his ski. As evident from steady measurement result, the stall angle is 35 to 40 deg, though it is hard to definitely define the stall angle owing to the three-dimensional nature of a jumper body. Similar results for the body angle of attack γ and the body forward leaning angle θ are shown in Fig. 3 (b) and (c) respectively. For these figures, the data were given also for an A-class and a high school jumpers. It is shown in Fig. 3 (b) that γ is larger for a high school jumper to result in larger drag due to his posture where it nearly stands up for airflow. It is seen in Fig. 3 (c) that θ values are not so different between the two jumps, though the flight distances are greatly different. However, the time t_f at which a flight entered a quasi-steady flight is different for the two flights. The jumping of A-class jumper enters the quasi-steady flight phase earlier than the high school jumper. In the initial phase before t_f , the body nearly stands up for airflow resulting in larger θ causing larger drag. A quick transition to the quasi-steady flight is desirable for a successful jumping flight.

3.2. Correlations between flight distance and jumper posture parameters

3.2.1. Reduced flight distance

It is understood that a jumper posture characterized by the angles, α , γ and θ influences the aerodynamic force coefficients, which, in turn, influences the flight distance. We investigate the correlations among them. One of the most important measures for the evaluation of jumping is the flight distance D_j , which is directly influenced by the take-off velocity U_0 . Therefore, the flight distance must be corrected by the effect of U_0 for comparison. The

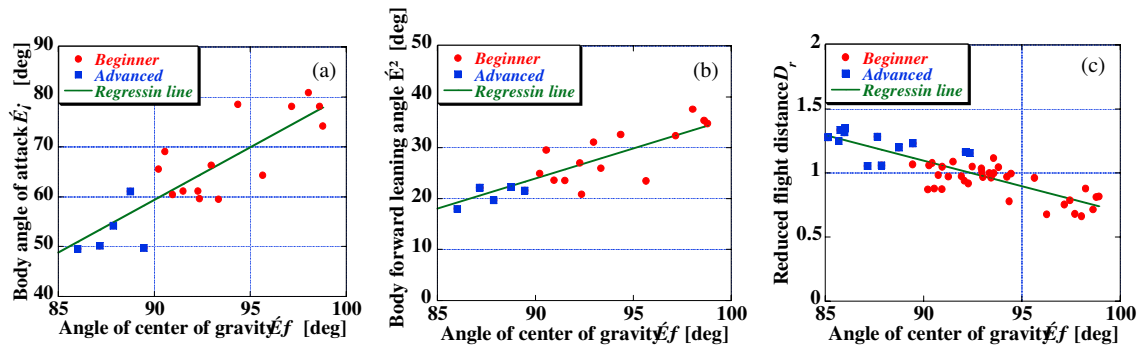


Fig. 5. Correlations, (a) for ζ - γ , (b) for ζ - θ and (c) for ζ - D_r correlations.

reference flight distance, D_v , is calculated as the free flight distance in vacuum as a function of U_0 . The dimensionless flight distance, D_r , is defined by $D_r = D/D_v$. The specification of the virtual jumping field for the calculation is: 11 deg. of downward angle around the take-off point, the height of the take-off point = 4 m, the angle of landing slope = 37.5 deg., and no less-steep entrance portion of landing slope. The result is that D_v is nearly in proportion to U_0 with larger increasing rate for higher U_0 : 83 m for $U_0 = 23$ m/s (=82.8 km/h), 103.5 m for $U_0 = 26$ m/s (= 93.6 km/h).

3.2.2. Correlation results: α - D_r , γ - D_r , θ - D_r and t_f - D_r correlations

The correlation results are shown in Fig. 4, (a) for α - D_r , (b) for γ - D_r , (c) for θ - D_r , and (d) for t_f - D_r . The values of α , γ , θ and t_f were measured at 1.4 s after take-off, when every flight has entered a quasi-steady flight phase. It is seen that the angles α , γ and θ should be smaller for larger D_r , as smaller α , γ and θ lead to smaller aerodynamic drag. The relation $\gamma = \theta + \alpha$ indicates that a flight with small θ is not always effective for large D_j if both α and γ are large, because this posture that is a typical one of beginners results in large drag. The result of Figure 4 (d) indicates that quick completion of initial movement subsequent to take-off is important for large D_j . In the initial phase before entering a quasi-steady flight a jumper body rather stands up for airflow resulting in larger θ causing larger drag. Quick transition to a quasi-steady flight is desirable for a long flight distance.

It is evident that every parameter, α , γ , θ and t_f is small for advanced jumpers in the initial phase of flight. This condition assures of small drag during flight. Furthermore, the data scattering of each parameter is small for advanced jumpers, which suggests that the flights of advanced jumpers are rather reproducible and, thus, they can surely complete two good jumps in a jumping competition. The data for advanced jumpers can be definitely distinguished from those of beginners for γ and θ , but the data distribution is rather multi-layered for α and t_f . However the data D_r of the advanced jumpers are always higher than those of the beginners for the same α and t_f values. It is suggested that considerable training is required in order to master a jumping posture of small γ and θ .

3.2.3. Effect of the angle of CG-boots line at take-off

For small γ , which is one of the keys for large D_j , nose-down moment is required at the instant of take-off. However, the direct measurement of the moment from the images is impossible because the motion of a jumper before the take-off point is not visible as jumpers are behind the safety board. Instead, we selected the angle between the slope line at the take-off point and the CG-boots line of a jumper, ζ , as a measure of the nose-down moment at the instant of take-off. The correlations are shown in Fig. 5 (a), (b) and (c) for ζ - γ , ζ - θ and ζ - D_r correlations. It is seen these correlations are strong, in particular very strong in ζ - γ correlation. This result means smaller ζ is a condition for smaller γ . For a flight with small γ , sufficient nose-down moment is necessary at take-off because the aerodynamic moment is very small in the air. This suggests very strong correlation between ζ and D_r . In fact, this is true as seen in Fig. 5 (c).

4. Conclusions

The conclusions of this study are summarized as follows:

1. The body angle of attack γ , the ski angle of attack α , the body forward leaning angle θ , and the transient time to a quasi-steady flight t_f should be all small for larger jumping flight distance, which is a necessary condition for small drag force, in particular in the initial flight phase. Among these parameters, γ is the most influential.

2. The distribution of these measurement data is clearly distinguished between advanced jumpers and beginners.

The data of advanced jumpers are found in the small value ranges, and furthermore the data scattering of advanced jumpers are smaller than those of beginners.

3. In the initial flight phase, small drag is a key for long flight distance.

Acknowledgements

This research was financially supported by the Grant-in-Aid for Scientific Research from the Japan Society for the Promotion of Science (19650167).

References

- [1] Tani I. and Mitsuishi, T. Aerodynamics of ski jumping. *Science* (Japanese edition), 1951; 117-152. (in Japanese)
- [2] Tani I. and Iuchi M. Flight-mechanical investigation of ski jumping. *Scientific study of skiing in Japan*. 1971; 35-53..
- [3] Seo K., Watanabe I. and Murakami M. Aerodynamic force data for a V-style ski jumping flight. *Sports Engineering* . 2004; **7-1**: 31-39.
- [4] Seo K., Murakami M. and Yoshida K. Optimal flight technique for V-style ski jumping. *Sport Engineering*. 2004; **7-2**: 97-104.
- [5] Murakami M., Hirai N., Seo K. and Ohgi Y. Aerodynamic forces computation from high-speed video image of ski jumping flight. *Proc. of Asia-Pacific Congress on Sports Technology*. 2007; 857-861.
- [6] Murakami M., Hirai N., Seo K. and Ohgi Y. Aerodynamic study of ski jumping flight based on high-speed video image. *Proc. 7th ISEA*. 2008;.
- [7] Chandler, R. F. Investigation of inertial properties of the human body. *Technical Report AMRL-74-137*, Wright Patterson Air Force Base, 1975.